Published OnlineFirst August 21, 2018; DOI: 10.1158/2326-6066.CIR-18-0056

Research Article

Cancer Immunology Research

A2AR Antagonism with CPI-444 Induces Antitumor Responses and Augments Efficacy to Anti–PD-(L)1 and Anti–CTLA-4 in Preclinical Models

Stephen B. Willingham, Po Y. Ho, Andrew Hotson, Craig Hill, Emily C. Piccione, Jessica Hsieh, Liang Liu, Joseph J. Buggy, Ian McCaffery, and Richard A. Miller

Abstract

Adenosine signaling through A2A receptors (A2AR) expressed on immune cells suppresses antitumor immunity. CPI-444 is a potent, selective, oral A2AR antagonist. Blockade of A2AR with CPI-444 restored T-cell signaling, IL2, and IFNγ production that were suppressed by adenosine analogues *in vitro*. CPI-444 treatment led to dose-dependent inhibition of tumor growth in multiple syngeneic mouse tumor models. Concentrations of extracellular adenosine in the tumor microenvironment, measured using microdialysis, were approximately 100–150 nmol/L and were higher than corresponding subcutaneous tissue. Combining CPI-444 with anti–PD-L1 or anti–CTLA-4 treatment eliminated tumors in up to 90% of treated mice, including restoration of immune responses in models that incompletely responded to anti–PD-L1 or anti–CTLA-4 monotherapy. Tumor growth was fully inhibited when mice with cleared tumors were later rechallenged, indicating that CPI-444 induced systemic antitumor immune memory. $CD8^+$ T-cell depletion abrogated the efficacy of CPI-444 with and without anti–PD-L1 treatment, demonstrating a role for $CD8^+$ T cells in mediating primary and secondary immune responses. The antitumor efficacy of CPI-444 with and without anti–PD-L1 was associated with increased T-cell activation, a compensatory increase in CD73 expression, and induction of a Th1 gene expression signature consistent with immune activation. These results suggest a broad role for adenosine-mediated immunosuppression in tumors and justify the further evaluation of CPI-444 as a therapeutic agent in patients with solid tumors. *Cancer Immunol Res; 6(10); 1136–49. ©2018 AACR.*

Introduction

Advances in the immunotherapy of cancer have produced complete, durable antitumor immunity in a subset of patients. Efficacy is limited in many patients by factors within the tumor microenvironment (TME) that inhibit immune cell infiltration and/or lead to suppressed antitumor immune responses (1). Extracellular adenosine is normally produced in response to such stimuli as infection or ischemia to restrain immune responses and protect host tissues from excessive damage (2–4). Emerging evidence suggests tumors exploit this inhibitory mechanism by generating adenosine in the TME to create an immunosuppressive niche that promotes tumor growth and metastasis (2, 5–8). Accordingly, adenosine signaling through adenosine receptors expressed on immune cells has been shown to suppress antitumor immunity and limit the efficacy of immunotherapy, chemotherapy, adoptive cell transfer therapies, and vaccines in preclinical models (4, 9, 10). Prior investigations have also revealed the critical role of adenosine in mediating resistance to chemotherapy and poor overall survival in patients with triple-negative breast cancer (10).

Adenosine can be generated in the TME by multiple mechanisms, including the sequential action of the ectonucleotidases CD39 and CD73. The coordinated activity of these enzymes converts ATP to AMP and finally to adenosine. While normal physiologic concentrations of adenosine are low, hypoxic conditions within the TME induce HIF-1α–dependent expression of the adenosinergic pathway (11–15). Adenosine may also be generated by infiltrating immune and stromal cells, including $CD39^+CD73^+$ regulatory T cells that convert ATP released from apoptotic cells to adenosine and further suppress antitumor immunity (16–18). Less common methods of generating or preserving extracellular adenosine in the TME include the release of intracellular adenosine from apoptotic cells, equilibrative and concentrative nucleotide transporters, direct generation by alkaline phosphatases, or downregulation of adenosine deaminase and its cofactor CD26 (19).

Extracellular adenosine exerts an immunosuppressive effect by signaling through the G_s-coupled A2A and A2B adenosine receptors (A2AR and A2BR; ref. 20). A2AR is the high-affinity adenosine receptor and appears to have the widest prevalence across immune cells within both the innate and adaptive systems (21). Previous studies have shown A2AR signaling inhibits the effector function of multiple immune subsets, including T cells and NK cells (13, 22–25). Genetic deletion of A2AR and synthetic A2AR antagonists have been reported to

Corvus Pharmaceuticals, Burlingame, California.

Note: Supplementary data for this article are available at Cancer Immunology Research Online (http://cancerimmunolres.aacrjournals.org/).

Corresponding Author: Stephen B. Willingham, Corvus Pharmaceuticals, 863 Mitten Road, Suite 102, Burlingame, CA 94010. Phone: 650-900-4527; Fax: 844-463-2039; E-mail: swillingham@corvuspharma.com

doi: 10.1158/2326-6066.CIR-18-0056

Published OnlineFirst August 21, 2018; DOI: 10.1158/2326-6066.CIR-18-0056

counteract adenosine immunosuppression and restore antitumor immunity (13, 26–32). Adenosine signaling through A2AR on tumor-infiltrating T cells may be a particularly important mechanism by which tumors escape immune destruction (13). Consequently, the therapeutic efficacy of A2AR antagonists may be maximized in "hot" tumors characterized by infiltrating tumor-reactive T cells that are otherwise rendered impotent by adenosine in the TME (33). Adenosine signaling through A2AR and A2BR also promotes tumor growth by facilitating angiogenesis through VEGF production (13, 34, 35). Adenosine antagonists may, therefore, not only restore antitumor immune responses, but also inhibit tumor growth by impeding adenosine-mediated neovascularization (13).

Here, we describe the antitumor immunomodulating effects of CPI-444, an oral antagonist of A2AR. The potency and selectivity of CPI-444 was characterized by radioligand binding and cAMP inhibition assays. CPI-444 was effective at limiting tumor growth and extending survival in several syngeneic mouse tumor models, as both a single agent and in combination with anti–PD-L1 and anti–CTLA-4. These results suggest a broad role for adenosine-mediated immunosuppression in tumors and justify the further evaluation of CPI-444 as a therapeutic agent in patients with solid tumors.

Materials and Methods

cAMP in primary human T cells

Fresh human peripheral blood mononuclear cells (PBMC) were purchased from AllCells (Alameda). T cells were isolated by negative selection with Dynabeads Untouched Human T cells kit (Life Technologies, catalog no. 11344D) according to manufacturer's instructions. Purified T cells were cultured in DMEM + 10% FBS + 1% penicillin/streptomycin with Dynabeads Human T-Activator CD3/CD28 (Life Technologies, catalog no. 11132D). Forty-eight hours after seeding, cells were triturated and Dynabeads were removed using magnetic selection. Cells were returned to culture for an additional 24 hours prior to assay to achieve low baseline cAMP. NECA [5′-(N-Ethylcarboxamido) adenosine, (Tocris, catalog no. 1691, 10^{-5} to 10^{-9} mol/L final concentration)] and CPI-444 (Corvus Pharmaceuticals, 1 μmol/L final concentration) were prepared in assay buffer (HBSS containing 5 mmol/L HEPES, 0.1% BSA, 10 μmol/L rolipram, pH adjusted to 7.4 with 0.5 mol/L NaOH) at 4× final concentration. A total of 2.5 μL NECA and 2.5 μL CPI-444 were added to each well of a white 384-well plate prior to addition of cells. T cells were washed one time in assay buffer and resuspended at 1×10^6 cells/mL in assay buffer. cAMP was measured using the LANCE Ultra cAMP kit (PerkinElmer, catalog no. TRF0262). Ulight anti-cAMP antibody was added to the cell suspension at 1:150. Five-microliter cell suspension was added to each well of a white 384-well plate containing agonist and antagonist. Plates were centrifuged for 30 seconds at 500 × *g* to collect cells and drug treatments at the bottom of the wells prior to incubation at room temperature for 10 minutes. 2× Eu-cAMP tracer solution was prepared in detection buffer provided with the LANCE Ultra cAMP kit. Ten microliters of 2× Eu-cAMP tracer was added to each well and plates were centrifuged for 30 seconds at 500 × *g* to collect volumes into the bottom of the well. Plates were incubated for 3 hours at room temperature protected from light prior to evaluation of TR-FRET signal. TR-FRET was measured with the EnVision MultiLabel reader system (Perkin Elmer). A standard curve was generated by preparing serial dilutions of cAMP standard provided with the LANCE Ultra cAMP kit. TR-FRET signal (665 nm) was plotted as a function of cAMP concentration. Concentrations of cAMP for experimental values were interpolated from the standard curve.

cAMP assay

Assays were performed with the Lance cAMP immunoassay kit (PerkinElmer, catalog no. AD0263) using 1.5 nmol/L NECA at Pharmaron. Normalized data from 10 independent experiments were fitted by nonlinear regression using GraphPad Prism.

CPI-444 radioligand binding

The ability of CPI-444 to displace radioligand binding from the four identified adenosine receptor subtypes (A1, A2A, A2B, and A3) was tested in CHO-K1 (A1, A3) or HEK293 (A2A, A2B) cells expressing human recombinant receptors. Cell membranes were incubated for 1.5 hours at 22°C with [^{3}H]-CGS-21680 (20 nmol/L, 30 Ci/mmol) in 50 mmol/L trishydroxymethylaminomethane (Tris)-HCl (pH 7.5; Sigma Aldrich) containing 10 mmol/L $MgCl_2$ (Sigma Aldrich) and adenosine deaminase (0.1 IU/mL, Sigma Aldrich). Nonspecific binding was determined with 300 μmol/L N6-cyclohexyladenosine (Sigma Aldrich). CPI-444 was tested at 11 duplicate concentrations for the adenosine A1 and A2A assays between 0.1 nmol/L and 10 μmol/L; and for adenosine A2B and A3 assays between 0.3 nmol/L and 100 μmol/L. Radioactivity remaining on the filters was determined by liquid scintillation spectrophotometry. Appropriate concentration ranges and radioligands used are summarized in Supplementary Table S1. The IC_{50} (concentration causing half-maximal inhibition of radioligand binding) was estimated by fitting a logistical equation to the observed concentration–response curves.

Inhibition of phosphorylated (p)CREB signaling

Fresh human PBMCs were purchased from AllCells (Alameda). Cells were cultured at a density of 10^7 cells/mL in RPMI1640 plus 10% FBS for the duration of the experiment. One-hundred microliters of cells were added per well (10^6 cells total). CPI-444 (1 μmol/L), control A2AR antagonist ZM 241385 (1 μmol/L, Tocris, catalog no. 1036), or DMSO vehicle control was added to each well of a 2.0 mL deep well polypropylene plate (Thermo Scientific catalog no. 278743 or Corning catalog no. P-DW-20-C), and cells were cultured for 1 hour at 37°C. NECA (1 μmol/L) was then added and cells were incubated for 1 hour at 37°C. Following stimulation, cells were fixed with 1.6% paraformaldehyde (Electron Microscopy Sciences, catalog no. 15710) for 10 minutes at 37°C. Cells were centrifuged 5 minutes at 1,000 × *g* and, following aspiration, were resuspended in 1-mL cold methanol and stored at −80°C for 1 day to 1 week. Cells were pelleted (1,000 × *g* for 5 minutes), washed twice with 1 mL of PBS (Life Technologies) + 1% BSA (Sigma Aldrich, catalog no. A2153) + 0.1% sodium azide (Sigma Aldrich, catalog no. S2002), and then 100 μL of the residual volume of cells was stained with an antibody cocktail containing anti-CD14 BV421(BioLegend, catalog no. 301830, 1 μL), anti-CD3 FITC (BD Biosciences, catalog no. 561807, 1.25 μL), anti-CD20 PE (BD Biosciences, catalog no. 561174, 1.25 μL), anti-CD4 APC-Cy7 (BD Biosciences, catalog no. 561839, 0.6 μL), anti-cPARP A700 (BD Biosciences, catalog no. 560640, 0.5 μL), anti-pCREB AF647 (Cell Signaling Technology, cat. no. 14001, 1 μL) for 1 hour at room temperature in the dark. Cells were then washed twice with FACS buffer and acquired on a

Published OnlineFirst August 21, 2018; DOI: 10.1158/2326-6066.CIR-18-0056

flow cytometer (Sony Cell Sorter SH800). Data were analyzed using FlowJo version 9. The reported CREB phosphorylation in each condition is normalized to the level in unstimulated cells (mean fluorescent intensity in stimulated condition ÷ mean fluorescent intensity in unstimulated condition)

Inhibition of phosphorylated (p)ERK signaling

PBMCs were purchased from AllCells and either used fresh or cryopreserved for future use. Fresh PBMCs were cultured at a density of 10^7 cells/mL, and cryopreserved cells were cultured at 2×10^6 cells/mL in RPMI plus 10% FBS for the duration of the experiment. Cryopreserved cells were gently thawed at 37°C, and then live cells were separated by overlaying 10 mL of cells on 4 mL Ficoll-Paque (GE Healthcare, catalog no. 17-5442-02), spinning at 400 × *g* for 30 minutes and collecting the cells at the interphase. One-hundred microliters of cells were added per well. CPI-444 (1 μmol/L), ZM 241385 (1 μmol/L), or DMSO vehicle control was added to each well of a deep-well plate, and cells were cultured for 1 hour at 37°C. NECA (1 μmol/L) was then added to appropriate wells, and cells were cultured for 45 minutes at 37°C. Biotinylated antibodies against anti-CD3 and anti-CD28 antibodies (3 μg/mL) were added to stimulate the cells for 13 minutes. The antibodies were crosslinked with avidin (50 μg/mL) for 2 minutes. Following stimulation, cells were fixed with 1.6% PFA for 10 minutes at 37°C. Cells were spun 5 minutes at 1,000 × *g* and, following aspiration, were resuspended in 1-mL cold methanol and stored at −80°C for 1 day to 1 week. Cells were spun out of methanol (1,000 × *g* for 5 minutes), washed twice with 1 mL of FACS buffer, and then 100 μL of residual volume of cells was stained with an antibody cocktail containing antibodies to CD14 (BioLegend, catalog no. 301830), CD3 (BD Biosciences, catalog no. 561807), CD8 (BD Biosciences, catalog no. 555367), CD4 (BD Biosciences, catalog no. 560649), cPARP (BD Biosciences, catalog no. 560640), and pERK (Cell Signaling Technology, catalog no. 13148S) for 1 hour at room temperature in the dark. Cells were then washed twice with FACS buffer and acquired on the flow cytometer (Sony Cell Sorter SH800). To quantify ERK phosphorylation, the percentage of T cells staining positive for phospho-ERK was determined by using the unstimulated condition to guide the gates for positivity.

IFNγ and IL2 analysis of human PBMCs

Buffy coat samples from healthy donors were purchased from the Stanford Blood Center. PBMCs were isolated using Histopaque-1077 (Sigma-Aldrich, catalog no. 10771) according to standard protocols. PBMCs were washed in autoMACS Rinsing Solution (Miltenyi Biotec, catalog no. 130-091-222) and resuspended in DMEM (Thermo Fisher Scientific, catalog no. 11965-118) containing 10% human serum (Sigma-Aldrich, catalog no. H4522). A total of 5×10^5 cells were incubated with 0.1 μmol/L, 1 μmol/L, or 10 μmol/L NECA or 0.1 μmol/L, 1 μmol/L, or 10 μmol/L CPI-444 in a U-bottom 96-well plate (VWR, catalog no. 10062-902) for 1 hour. T cells were then activated with Dynabeads Human T-Activator CD3/CD28 (Thermo Fisher Scientific, catalog no. 11132D) at a 1:3 cells: beads ratio. Forty-eight hours later, 5 μL of cell-free supernatant was collected and assayed for IFNγ or IL2 using the AlphaLISA kit (Perkin Elmer, catalog no. AL217F or AL221F). Data were analyzed with an EnVision Multilabel Plate Reader (Perkin Elmer). CGS-21680 used in experiments shown in Supplementary Fig. S1B was from Tocris (catalog no. 1063).

Cells

MC38 cells were obtained from an external collaborator. CT26, RENCA, and B16 tumor cell lines were obtained from the ATCC. The identity and specific pathogen–free (including *Mycoplasma*) status of these cells was validated by microsatellite genotype analysis (IDEXX Bioresearch). MC38 cells were cultured in DMEM + 10% FBS (VWR). CT26 cells were cultured in RPMI1640 (ATCC, catalog no. 30-2001) + 10% FBS (VWR). RENCA cells were cultured in RPMI (Thermo Fisher, catalog no. 61870-127) + 10% FBS (VWR) + 0.1 mmol/L MEM nonessential amino acids (Thermo Fisher, catalog no. 11140-050) + 1 mmol/L sodium pyruvate (Sigma Aldrich, catalog no. S8636). 1% penicillin–streptomycin solution (Thermo Fisher, catalog no. 15140122) was added to all culture media. Cell lines were typically cultured three generations prior to use.

Mice

All animal studies were conducted in accordance with an Institutional Animal Care and Use Committee. Six- to 8-week-old C57BL/6 and Balb/c mice were purchased from Charles River. Mice were typically housed in the vivarium (Corvus Pharmaceuticals) for two weeks prior to tumor cell injection. Mice used in the *in vivo* microdialysis procedure were housed and implanted with tumors at Charles River Laboratories. See Supplementary Table S2 for additional details regarding the setup and dosing of animal models.

Tumor engraftment

Tumor cells were typically prepared in 100-μL cold PBS in a microfuge tube. A 31-gauge needle was used to perform a subcutaneous injection of cells onto the lower back region of syngeneic mice. See Supplementary Table S2 for additional details regarding the setup and dosing of animal models. Caliper measurement was performed every 2–4 days using a digital caliper (Fowler–Sylvac). Tumor volume was calculated using the formula $(\text{length} \times \text{width}^2)/2$.

CPI-444 treatment

A 10 mg/mL stock was prepared in 40% hydroxypropyl β-cyclodextrin in 0.1 N hydrochloric acid, mixed on a stirrer plate, and filtered through a 0.45-μm filter. The solution was adjusted with 1.0 N sodium hydroxide and 1.0 mol/L citric acid to pH 3-4. A 10 mg/mL stock solution was further diluted into lower concentration: 1 mg/mL and 0.1 mg/mL.

Flow cytometry

Spleens and tumors were harvested at day 15 post-implantation of 10^6 MC38 cells. Single-cell suspensions were prepared mechanically using a 3-mL syringe plunger pushing the tumor or organ through a 70-μm filter. Red blood cells in the spleens were lysed using ACK Lysis Buffer (Life Technologies, catalog no. A10492-01). Live/Dead cell discrimination was performed using Live/Dead Fixable Violet Dead Cell Stain kit (Life Technologies), according to the manufacturer's protocol. Cell surface staining was done for 20–30 minutes. Intracellular staining was done using a fixation/permeabilization kit (FOXP3 Fix/Perm Kit, BioLegend, catalog no. 126408). Antibodies used include: anti-CD45 (BioLegend, catalog no. 103116), anti-CD4 (BioLegend, catalog no. 100540), anti-CD8 (BioLegend, catalog no. 100540), anti-CD3 (BioLegend, catalog no. 100216), anti–PD-1 (BioLegend, catalog. no. 124321), anti-GITR (BioLegend,

Published OnlineFirst August 21, 2018; DOI: 10.1158/2326-6066.CIR-18-0056

catalog no. 120222), anti-LAG3 (eBioscience, catalog no. 11-2231-82), anti-CD127 (BioLegend, catalog no. 135033), and anti-IFNγ (BioLegend, catalog no. 505831). All flow cytometric analysis was done using Cytoflex (Beckman Coulter) and analyzed using FlowJo software (TreeStar).

CD73 IHC

After routine deparaffinization and rehydration, antigen retrieval was performed using a Dako Target Retrieval and a Dako Pascal pressure chamber. After a 30-minute application of blocking solutions (vendor unknown) and rinsing, the primary antibody (CD73; clone D7F9A, Cell Signaling Technology) was applied at a 1:200 dilution for one hour. Polyclonal rabbit IgG, adjusted to the equivalent protein concentration as the primary antibody, was used as the negative isotype control. MACH 3 HRP Polymer (Biocare Medical) and Betazoid DAB (Biocare Medical) were used for detection. Sections were counterstained with Mayer hematoxylin. Each stained histologic section of tumor (test sample) was assessed microscopically and scored according to the intensity of the appropriate compartmental staining (no staining = 0, weak staining = 1, moderate staining = 2, strong staining = 3) and the extent of stained cells (0% = 0, 1%–10% = 1, 11%–50% = 2, 51%–80% = 3, 81%–100% = 4). The final score for each test sample was determined by multiplying the intensity score with the extent score of stained cells, with a minimum score of 0 and a maximum score of 12. Staining on endothelial cells was excluded from the assessment presented in Fig. 6C. Photomicrographs were taken on an Olympus BX-41 brightfield microscope using Olympus DP Controller and DP Manager software.

In vivo microdialysis procedure

In vivo microdialysis and adenosine quantification were performed by Charles River Laboratories. Briefly, microdialysis probes were implanted into tumors or healthy contralateral subcutaneous tissue when tumors were approximately 200–300 mm^3. Microdialysis was performed one day after surgery at a flow rate of 1.5 μL/minute using perfusion fluid composed of 147 mmol/L NaCl, 3.0 mmol/L KCl, 1.2 mmol/L $CaCl_2$, and 1.2 mmol/L $MgCl_2$, omitting inhibitors of adenosine metabolism and transport. Concentrations of adenosine were determined by HPLC with tandem mass spectrometry detection in positive ionization mode using an API 4000 triple quadrupole (Applied Biosystems) equipped with a Turbo Ion Spray interface. Data were calibrated and quantified using the Analyst data system (Applied Biosystems, version 1.4.2).

NanoString analysis of MC38 tumors

Tumor excision was performed on MC38 tumor–bearing mice treated with either anti–PD-L1 or anti–PD-L1 + CPI-444 nine days after the treatment initiation. See Supplementary Table S2 for additional details regarding the setup and dosing of animal models. Tumors were kept in RNAlater Stabilization Solution (Thermo Fisher Scientific, catalog no. AM7021) at 4 degree. RNA extraction was done within a week post tumor excision using RNeasy Mini Kit from (Qiagen, catalog no. 74106). Extraction was done according to the manufacturer's protocol. Mouse Cancer Immune Panel (NanoString, catalog no. XT-CSO-MIP1-12) along with a custom codeset consisting of probes to Adk, Adm, Adora2b, Adora3, Apobec3, Bbc3, Bnip3, Ccnd2, Cnr1, Cnr2, Drd2, Drd3, Drd4, Epas1, Epo, Fosl1, Grm5, Nr4a1, Nr4a2, Nt5c1a, P2rx7, Panx1, Pgk1, Pten, Slc28a2, Slc29a1, Slc29a2, Slc2a1, and Usp4 was used. All steps were done according to the NanoString's protocol. Data were analyzed using nSolver Analysis Software version 2.6

Results

CPI-444 is a potent and selective A2AR antagonist

CPI-444 is a synthetic, non-xanthene small molecule with a molecular weight of 407.43 (Fig. 1A). The ability of CPI-444 to displace radioligand binding to the four identified adenosine receptor subtypes (A1, A2A, A2B, and A3) was tested with human recombinant receptors expressed in mammalian cell lines (Supplementary Table S1). CPI-444 bound A2A receptors with a K_i of 3.54 nmol/L and demonstrated a greater than 50-fold selectivity for the A2A receptor over other adenosine receptor subtypes (Fig. 1B). Adenosine signaling through A2AR induces cAMP production (13, 21). Inhibition of cAMP production resulting from stimulation with the high-affinity, stable adenosine analogue NECA (5′-*N*-Ethylcarboxamidoadenosine) is frequently used as readout for activity of A2AR antagonists (21, 36). Notably, NECA is a much more potent agonist of A2AR and A2BR (A2AR K_i = 20 nmol/L, A2BR EC_{50} = 330 nmol/L) than adenosine (A2AR K_i = 700 nmol/L, A2BR EC_{50} = 24000 nmol/L; ref. 21). The ability of CPI-444 to functionally antagonize A2AR and block adenosine-mediated cAMP induction was investigated using HEK-293 cells that stably overexpress A2AR. CPI-444 blocked the induction of cAMP by 1.5 nmol/L NECA with an IC_{50} of 17.03 nmol/L (Fig. 1C).

CPI-444 restores T-cell activation *in vitro*

Activated T cells have high expression of A2AR, and NECA-mediated activation of A2AR increased cAMP in human T cells (Fig. 2A), consistent with previous reports (13, 36–38). Inclusion of CPI-444 led to a dose-dependent inhibition of the production

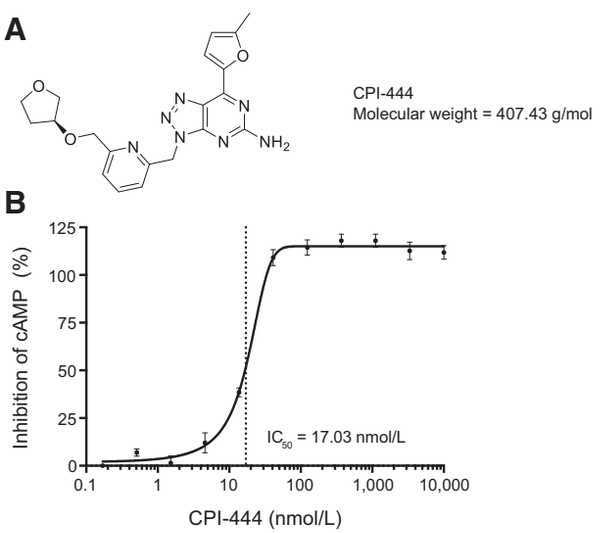

Figure 1.
CPI-444 is a potent and selective A2AR inhibitor. **A,** Structure and molecular weight of CPI-444. **B,** cAMP induction by NECA (1.5 nmol/L) in HEK-293 cells stably overexpressing A2AR and treated with CPI-444 (0.1 nmol/L–10,000 nmol/L).

Published OnlineFirst August 21, 2018; DOI: 10.1158/2326-6066.CIR-18-0056

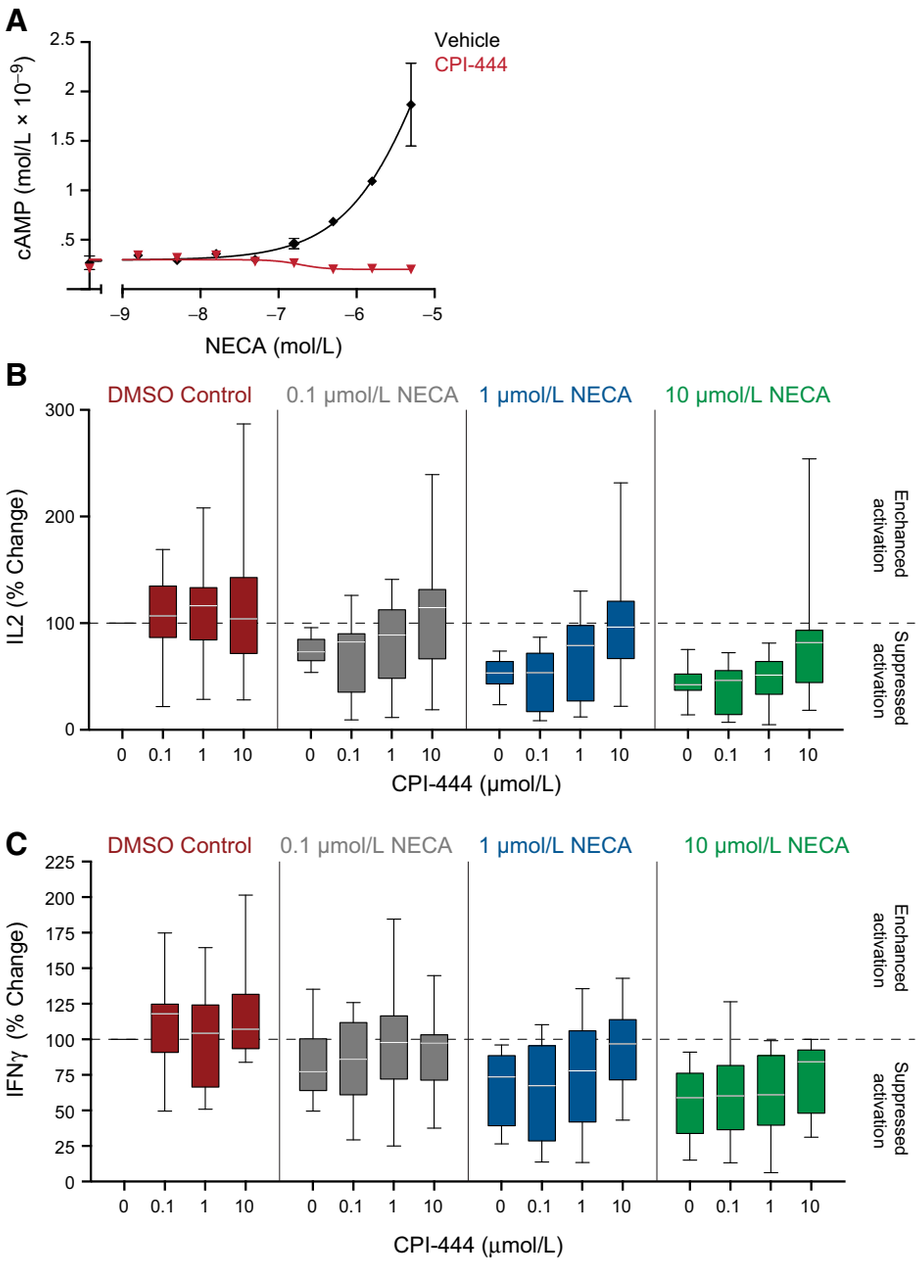

Figure 2.
CPI-444 restores T-cell activation. **A,** CPI-444 blocks the production of cAMP in primary human T cells upon A2AR stimulation with NECA. **B** and **C,** NECA (0.1, 1, or 10 μmol/L) suppressed release of the IL2 and IFNγ from activated human PBMCs ($n = 15$), mimicking the immunosuppressive effects of adenosine signaling. Blockade of A2AR with CPI-444 (0.1, 1, or 10 μmol/L) restored IL2 and IFNγ secretion back to levels observed in the absence of NECA signaling (DMSO control). Samples were analyzed 48 hours after stimulation. The median value is represented by a white line within the box, and the whiskers indicate the 5–95 percentile. Repeated measures analysis of the relationship between the percent inhibition of either IL2 or IFNγ to increases in CPI-444 was used to determine significant positive slopes (IL2 $P = 0.01$, IFNγ $P = 0.03$).

of intracellular cAMP following stimulation of activated primary human T cells with NECA ($IC_{50} = 70$ nmol/L; Fig. 2A). CPI-444 completely inhibited NECA-mediated elevation of cAMP in these human PBMC cultures, suggesting that A2AR is the dominant adenosine receptor that mediates immune suppression in this system. Elevated intracellular cAMP following A2AR activation results in the phosphorylation of CREB (cAMP response element-binding protein; ref. 39). CPI-444 treatment inhibited phosphorylation of CREB (pCREB; Supplementary Fig. S1A) in NECA-stimulated cells. These results demonstrate that CPI-444 restores T-cell signaling in the presence of adenosine analogues.

We next sought to determine whether CPI-444 abrogated the immunosuppressive effects of adenosine on T-cell activation and Th1 cytokine release. Th1 cytokines such as IL2 and IFNγ stimulate the differentiation and activation of cytotoxic lymphocytes that are responsible for the cell-mediated immune responses against viruses and tumor cells. IL2 is expressed by activated T cells, but not resting T cells, making it a surrogate for T-cell activation. Primary human PBMCs ($n = 15$ donors) were cultured in the presence of NECA (0.1, 1, or 10 μmol/L) to simulate the effects of adenosine on immune cell function. T cells were then activated for 48 hours. NECA suppressed release of IL2 (Fig. 2B) and IFNγ (Fig. 2C) in a concentration-dependent manner, mimicking the immunosuppressive effects of adenosine signaling. Antagonism of A2AR with CPI-444 (0.1, 1, or 10 μmol/L) inhibited the immunosuppressive effects of NECA and restored IL2 and IFNγ secretion back to or above that observed in the absence of NECA signaling (DMSO

Published OnlineFirst August 21, 2018; DOI: 10.1158/2326-6066.CIR-18-0056

control) in most instances. Similar results were observed in separate donors using a second A2AR agonist, CGS-21680 (A2AR K_i = 27 nmol/L, A2BR EC_{50} = 361,000 nmol/L; Supplementary Fig. S1B; ref. 21). To investigate the intracellular mechanism of NECA-mediated T-cell suppression, the activated, phosphorylated form of extracellular signal-regulated kinase (pERK) was measured following T-cell receptor (TCR) activation. Pretreatment of PBMCs with NECA inhibited pERK induction by TCR cross-linking, and CPI-444 fully restored pERK induction (Supplementary Fig. S1C). These results showed that restoration of T-cell function may be an important mechanism by which CPI-444 enables an antitumor response *in vivo*.

In vivo tumor efficacy of CPI-444 and tumor adenosine

MC38 is a mouse colon carcinoma cell line that is responsive to immune checkpoint blockade, including anti–PD-1 antibodies (28, 29). To evaluate the antitumor efficacy of CPI-444 *in vivo*, we engrafted MC38 cells onto the backs of syngeneic C57BL/6 mice. One day after tumor cell engraftment, vehicle control solution or CPI-444 (1, 10, or 100 mg/kg) was administered daily via oral gavage for 28 days (see Supplementary Table S2 for details of all animal experiments). Administration of CPI-444 at 10 mg/kg and 100 mg/kg resulted in a significant inhibition of tumor growth, whereas 1 mg/kg had no discernable effect compared with vehicle-treated animals (Fig. 3A and

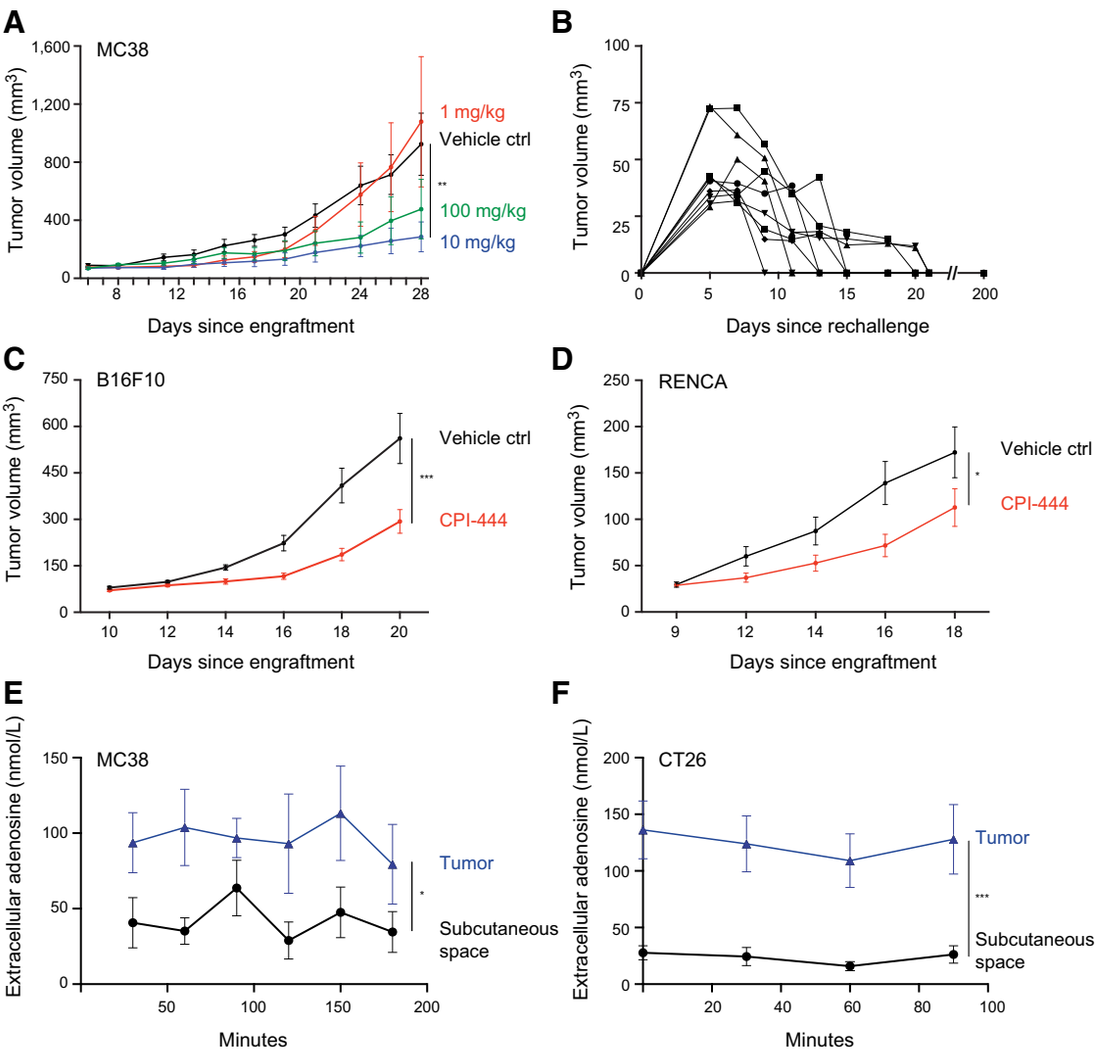

Figure 3.

CPI-444 induces long-term antitumor immunity. **A,** Tumor growth in C57BL/6 mice (n = 9–10 per group) treated with CPI-444 at the indicated concentrations after subcutaneous injection of 10^6 MC38 cells. Tumor growth was monitored every 2–4 days as indicated in the figure. **B,** 9 mice that achieved complete tumor growth inhibition were rechallenged with a new engraftment of 10^6 MC38 tumor cells. Tumors were assessed every 2–3 days over the following 15 days. **C,** CPI-444 (100 mg/kg) inhibits the growth of B16F10 tumors 10 days after injecting 2.5×10^5 cells. **D,** CPI-444 (10 mg/kg) inhibits the growth of RENCA tumors 10 days after injecting 2×10^5 cells. **E** and **F,** Concentration of extracellular adenosine over the indicated times in MC38 (n = 8; **E**) and CT26 (n = 7; **F**) tumors or healthy contralateral subcutaneous tissue when tumors were approximately 200–300 mm^3, as measured by microdialysis. Error bars, SEM. Significance was calculated using two-way ANOVA (*, $P < 0.05$; **, $P < 0.01$; ***, $P < 0.001$).

Published OnlineFirst August 21, 2018; DOI: 10.1158/2326-6066.CIR-18-0056

Supplementary Fig. S2A–S2C for spider plots of individual mice). Complete tumor regression was observed in 9 of 29 mice treated with CPI-444 (Supplementary Fig. S2D). These mice were evaluated by macroscopic examination and direct palpation for tumor recurrence for an additional 6 weeks after dosing was terminated. No tumor growth was observed, indicating that the tumor had been fully eliminated. To determine whether the immune response initiated by CPI-444 treatment resulted in a long-term memory response against tumor antigens, we rechallenged these mice with a new engraftment of MC38 tumor cells. Modest tumor growth was observed in the first 5 days after rechallenge. However, the tumors were fully rejected in all 9 rechallenged mice over the following 30 days (Fig. 3B). These mice were monitored for signs of tumor recurrence for an additional 100 days, but no tumor growth was observed in any animal. Tumor elimination occurred in the absence of any additional CPI-444 treatment. These results demonstrate that A2AR blockade with CPI-444 can elicit durable systemic immune memory without provoking the problematic activation-induced cell death (AICD) reported in studies utilizing A2AR-deficient T cells (40). CPI-444 treatment resulted in a similar inhibition of tumor growth in the B16F10 melanoma (100 mg/kg, Fig. 3C) and RENCA renal cell cancer syngeneic models (10 mg/kg, Fig. 3D).

We next aimed to determine whether extracellular adenosine concentrations in the TME correlated with the efficacy of CPI-444. CPI-444 has single-agent activity in the MC38 tumor model (Fig. 3A and B), but not in the CT26 model (Fig. 4C and D). Microdialysis probes were surgically implanted into established MC38 or CT26 tumors or healthy contralateral subcutaneous tissue as a control. Free interstitial adenosine was collected in live animals by microdialysis 24 hours later and measured by HPLC-coupled tandem mass spectrometry. Elevated adenosine concentrations were detected in the tumor microenvironment of MC38 tumors ($n = 8$) compared with the healthy contralateral subcutaneous tissue (Fig. 3E). A similar elevation of adenosine was detected in established CT26 ($n = 7$) tumors (Fig. 3F). Free extracellular adenosine was approximately 120–150 nmol/L in the tumors of both cell lines (Fig. 3E and F), suggesting the concentration of adenosine alone does not predict CPI-444 efficacy in MC38 and CT26 tumors.

CPI-444 treatment was well-tolerated in all mouse tumor models. A transient increase in activity and diarrhea was observed at high doses of CPI-444 (100 mg/kg) in Balb/c mice, but not in C57BL/6 mice. A moderate weight loss was observed in the RENCA model following CPI-444 treatment. These observations do not appear to be related to drug exposure (Supplementary Table S3) and may represent an inherent differential sensitivity to CPI-444 between the two strains. CPI-444 (1 pmol/L–10 μmol/L) did not impact tumor cell proliferation *in vitro* (Supplementary Fig. S2E and S2F), suggesting that CPI-444 efficacy observed *in vivo* is unlikely due to a direct effect on tumor cells.

CPI-444 enhances anti–PD-L1 and anti–CTLA-4 efficacy in syngeneic mouse tumor models

We evaluated the efficacy of CPI-444 when administered in conjunction with a blocking mAb against PD-L1. CPI-444 (100 mg/kg) treatment alone produced a statistically significant, but incomplete, inhibition of established MC38 tumor growth (Fig. 4A). Similar tumor growth inhibition was observed in mice treated with anti–PD-L1 (Fig. 4A). In contrast, administration of CPI-444 and anti–PD-L1 in combination stabilized or eliminated tumors in 5 of 10 mice (Fig. 4A and B). Similar results were observed when CPI-444 was combined with anti–PD-1 in the CT26 model. Administration of anti–PD-1 or CPI-444 (1 mg/kg) did not significantly inhibit tumor growth. However, CPI-444 treatment in combination with anti–PD-1 did inhibit tumor growth and improved overall survival for more than 3 weeks following the last dose of CPI-444 or anti–PD-1 antibody (Fig. 4C and D).

The efficacy of CPI-444 and anti–CTLA-4 treatment was also evaluated in the MC38 and CT26 tumor models. Combining CPI-444 (100 mg/kg) with anti–CTLA-4 synergistically inhibited the growth of established MC38 tumors (Fig. 4E), leading to complete tumor elimination in 100% of treated mice (Supplementary Fig. S3A). Dual blockade of A2AR and CTLA-4 was also more effective than either monotherapy in the CT26 model. CPI-444 (10 mg/kg) potentiated the efficacy of anti–CTLA-4 at both 100 μg (Fig. 4F) and 50 μg (Supplementary Fig. S3B) doses.

Prior attempts to combine anti–PD-1 and anti–CTLA-4 antibody therapy have resulted in enhanced clinical activity, but also increased incidence of treatment-related adverse events in patients with melanoma (41, 42). We hypothesized that A2AR blockade with CPI-444 would enable lower doses of antibody in anti–PD-1 and anti–CTLA-4 combinations, while preserving the enhanced efficacy. A triple-combination experiment was performed wherein CPI-444 (10 mg/kg), anti–PD-1 (25 μg/dose), and anti–CTLA-4 (25 μg/dose) were administered at low doses. CPI-444 and anti–PD-1 lost single-agent efficacy at these doses. However, established CT26 tumors were still fully eliminated in 5 of 10 mice treated with the triple combination compared with 30% of mice in the second best treatment doublet of CPI-444 plus anti–CTLA-4 (Fig. 4G and H). These results suggest that blockade of the adenosine pathway may be important for enhancing antitumor responses and limiting toxicity in solid tumors that show an incomplete response to anti–PD-L1 or anti–CTLA-4 therapy.

CPI-444 enhances T-cell activation and antitumor immunity *in vivo*

Flow cytometry was performed on MC38 tumors treated with CPI-444 with and without anti–PD-L1 to characterize the effects of CPI-444 on antitumor immune responses. The efficacy of CPI-444 in combination with anti–PD-L1 was associated with increased T-cell infiltration (Fig. 5A). CPI-444 antagonism of adenosine signaling increased IFNγ production in $CD8^+$ T cells (Fig. 5B). An increase in GITR and IL7Rα expression was also observed on T cells (Fig. 5C and D). GITR has low expression on resting T effector cells but is quickly upregulated following T-cell activation, whereas IL7Rα expression is a marker of memory T cells. We also observed evidence of immune activation in the periphery, as CPI-444 treatment increased the frequency of $CD8^+PD\text{-}1^+$ splenocytes (Fig. 5E). This increased immune response was associated with smaller MC38 tumors (Fig. 5E). CPI-444 also increased the expression of LAG3 on $CD8^+$ splenocytes (Fig. 5F). LAG3 is upregulated following T-cell stimulation as part of a compensatory inhibition mediated through interactions with MHC class II. In total, these observations suggest that

Published OnlineFirst August 21, 2018; DOI: 10.1158/2326-6066.CIR-18-0056

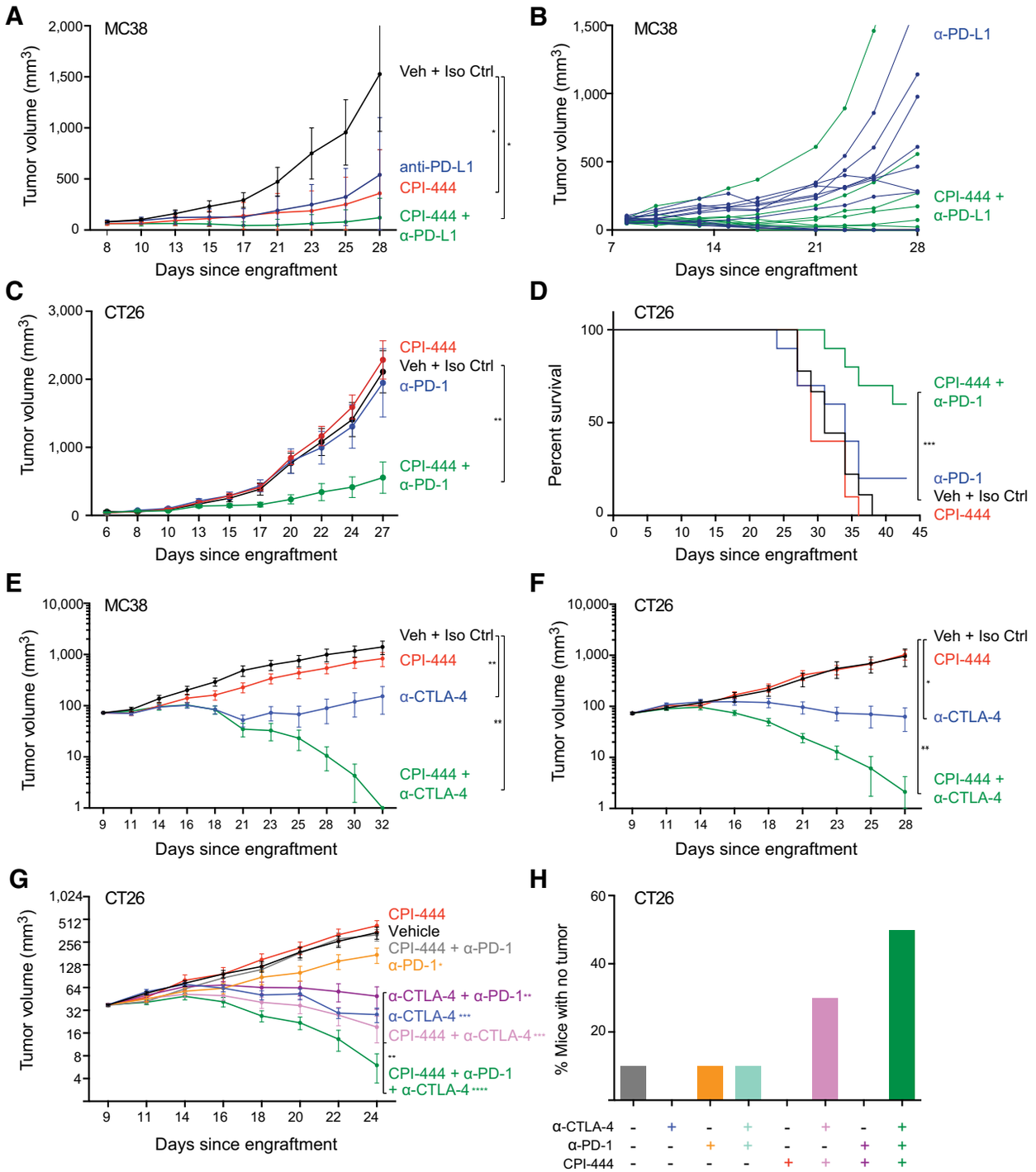

Figure 4.

CPI-444 synergizes with anti–PD-L1 and anti–CTLA-4 treatment. **A** and **B,** Anti–PD-L1 (200 μg, $n = 10$) or CPI-444 (100 mg/kg, $n = 10$) monotherapy resulted in an incomplete inhibition of MC38 tumor growth, while administration of CPI-444 (100 mg/kg) in combination with anti–PD-L1 (200 μg) stabilized or eliminated tumors in 5 of 10 mice. **C** and **D,** Administration of CPI-444 (1 mg/kg) in combination with anti–PD-1(100 μg) inhibits the growth of CT26 tumors ($n = 10$; **C**), resulting in improved overall survival (**D**). **E** and **F,** CPI-444 treatment in combination with anti–CTLA-4 (100 μg) successfully eliminated tumors in MC38 (100 mg/kg; **E**) and CT26 (10 mg/kg; **F**) tumor models ($n = 10$/group). **G,** CPI-444 (10 mg/kg) treatment combined with subtherapeutic doses of anti–CTLA-4 (25 μg) and anti–PD-1 (25 μg) induced a rapid regression in the CT26 tumor model ($n = 10$/group). **H,** Approximately two weeks after treatment initiated, the combination of all three treatments successfully eliminated tumors in 5 of 10 mice. Error bars, SEM. Significance was calculated using two-way ANOVA, except in **D,** which was calculated with log-rank (Mantel–Cox) test (*, $P < 0.05$; **, $P < 0.01$; ***, $P < 0.001$).

Published OnlineFirst August 21, 2018; DOI: 10.1158/2326-6066.CIR-18-0056

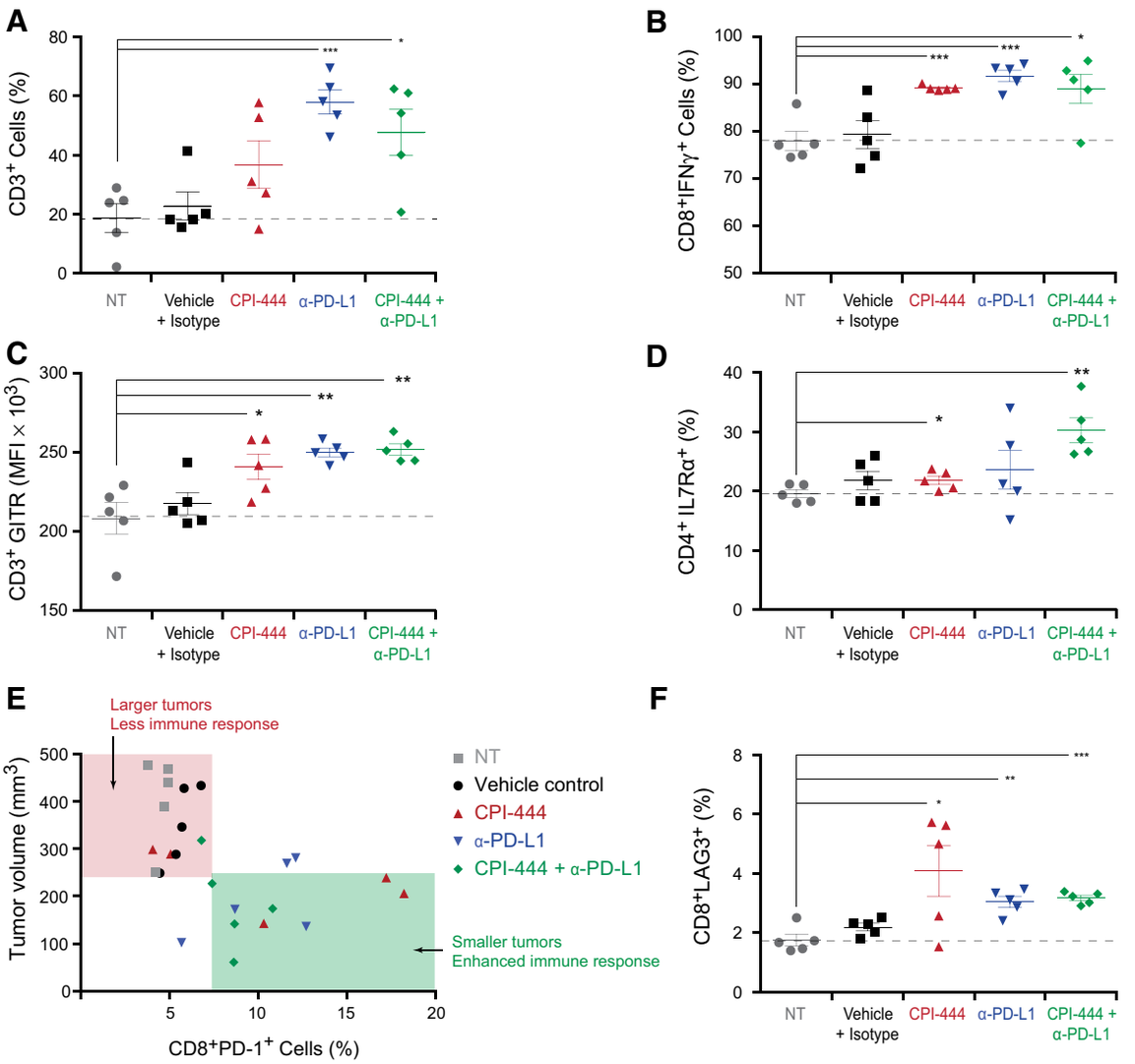

Figure 5.

CPI-444 enhances T-cell activation in MC38 tumors. **A,** T-cell infiltration into MC38 tumors is increased following treatment with CPI-444 in combination with anti–PD-L1. Data were gated on $CD45^+$ cells. **B,** IFNγ production in $CD8^+$ T cells is increased by CPI-444 alone and in combination with anti–PD-L1. **C,** CPI-444 and anti–PD-L1 increase GITR expression on $CD45^+CD3^+$ T cells. **D,** CPI-444 increases the frequency IL7R expression on $CD4^+$ T cells. **E,** Increased frequency of $CD8^+PD\text{-}1^+$ splenocytes in CPI-444 plus anti–PD-L1–treated mice is associated with smaller tumors. **F,** CPI-444 increases the frequency of $CD8^+Lag3^+$ T cells. Data were gated on the $CD45^+CD3^+$ population in the spleen. Significance was calculated using *t* tests (*, $P < 0.05$; **, $P < 0.01$; ***, $P < 0.001$). Each symbol represents an individual mouse tumor or spleen in all data plots. CPI-444 (100 mg/kg) and anti–PD-L1 (200 μg) were used in all experiments shown here.

CPI-444 enhances T-cell activation in both the periphery and tumor microenvironment.

Antitumor efficacy of CPI-444 requires $CD8^+$ cells

Previous studies have highlighted the role of adenosine signaling in protecting tumors from T-cell–mediated clearance (13, 43). Antibody-mediated depletion of $CD8^+$ cells in tumor-bearing mice prior to treatment abolished the efficacy of CPI-444 alone (Fig. 6A, left) and in combination with anti–PD-L1 (Fig. 6A, right). Depletion of $CD4^+$ cells had minimal effect on efficacy (Fig. 6A). These results demonstrate the essential contribution of $CD8^+$ T cells in mediating primary and secondary immune responses following A2AR blockade.

A2AR blockade induces a compensatory increase in CD73 expression

CPI-444 inhibits the growth of established MC38 tumors (Figs. 4A and E and 6A), but these tumors are not typically fully eliminated with single-agent treatment alone. Further elevation of adenosine in the TME through increased CD73 expression represents a potential resistance mechanism by which tumors could overwhelm A2AR antagonism. We observed a significant increase in the frequency and intensity of CD73 expression in MC38 tumors following treatment with CPI-444 (Fig. 6B; Supplementary Fig. S4A and S4B for images depicting specificity of anti-CD73). Anti–PD-L1 treatment also increased CD73 expression in MC38 tumors (Fig. 6B), as well as on splenocytes collected

Published OnlineFirst August 21, 2018; DOI: 10.1158/2326-6066.CIR-18-0056

from tumor-bearing mice (Fig. 6C). Adenosine generated by this compensatory increase in CD73 expression may restore immunosuppression and, thereby, restrict the efficacy of A2AR inhibitors and anti–PD-L1 treatment. Future studies will determine whether dual blockade of A2AR and CD73 neutralizes this potential resistance mechanism and enables a more robust antitumor response.

Gene expression changes associated with combination CPI-444 and anti–PD-L1 efficacy

We assessed gene expression changes associated with therapeutic response to combination CPI-444 and anti–PD-L1 treatment in MC38 tumors. Combined CPI-444 plus anti–PD-L1 treatment cleared approximately 90% of established MC38 tumors (Fig. 6A). We treated more than 50 MC38 tumor-bearing mice with CPI-444 and anti–PD-L1 to generate 5 tumors that were nonresponsive to treatment. RNA was purified from tumors excised at day 17, a time at which both responding and nonresponding ($n = 5$/each) tumors were still present (Fig. 7A). Gene expression was assayed using the NanoString PanCancer Immune Profiling Panel and a custom adenosine-related codeset. An aggregate T-effector signature consisting of genes for CD8a, CXCL9, CXCL10, EOMES, IFNγ, GZMA, GZMB, and TBX21 was higher in responding tumors, consistent with an activated T-cell–mediated antitumor response (Fig. 7B). Immune checkpoints, such as genes for PD-L1, LAG3, TIGIT, CD40, and GITR (TNSRSF18), were expressed in responding tumors, suggesting possible mechanisms of adaptive resistance and feedback inhibition (Fig. 7B). The expression of genes for CFI and NT5C1a was higher is nonresponders (Fig. 7B). The role of these genes in mediating resistance to combination CPI-444 and anti–PD-L1 is currently unknown, but the 5′ nucleotidase NT5C1a could contribute to additional adenosine generation in the TME following its extracellular release from dying cells. Caution must be applied in interpreting these results. Although individual genes were significantly different between groups, the relatively small number of total samples ($n = 10$) caused all genes to lose statistical significance after adjustments for multiple testing (Supplementary Table S4 for raw and corrected P values).

Discussion

Elevated extracellular adenosine within the TME suppresses antitumor immune responses. Here, we showed that blockade of A2AR with CPI-444 can neutralize adenosine signaling and restore antitumor immunity. CPI-444 treatment alone and in combination with anti–PD-1, anti–PD-L1, and anti–CTLA-4 induced T-cell–mediated antitumor responses, inhibited tumor

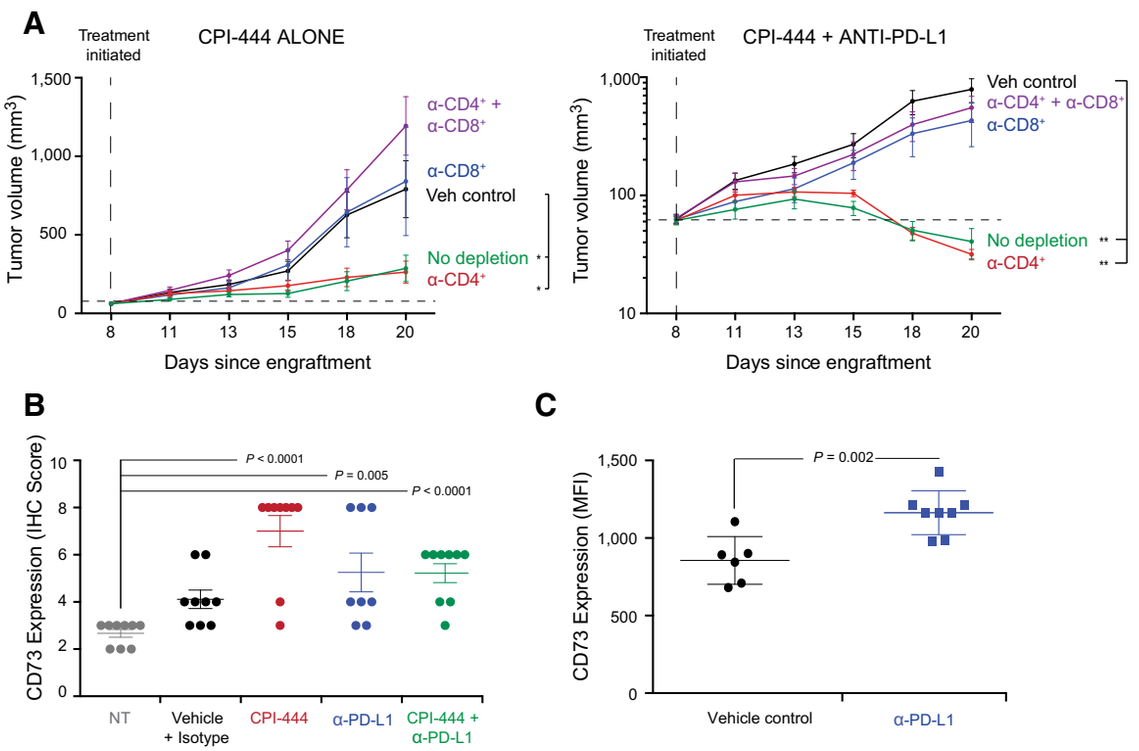

Figure 6.

CPI-444 efficacy requires CD8$^+$ T cells and is associated with increased CD73 expression. **A,** Depletion of CD8$^+$ T cells prior to CPI-444 monotherapy (100 mg/kg, left) or CPI-444 (100 mg/kg) + anti–PD-L1 (200 μg) combination treatment (right) abolishes antitumor efficacy in the MC38 tumor model. Anti-CD4 (clone GK1.5, 100 μg) and anti-CD8 (clone 53-6.72, 500 μg) were used for depletion of CD4$^+$ and CD8$^+$ subsets. **B,** CD73 expression was significantly higher in MC38 tumors treated with CPI-444 (100 mg/kg) + anti–PD-L1 (200 μg) relative to controls. CD73 was assessed by IHC and scored as a composite of frequency of expression × intensity of expression (scale: 1–5). Endothelial cell staining was excluded from the assessment. **C,** Anti–PD-L1 (200 μg) treatment increased CD73 expression on splenocytes from MC38 tumor–bearing mice. Significance was calculated using two-way ANOVA (*, $P < 0.05$; **, $P < 0.01$; ***, $P < 0.001$).

Published OnlineFirst August 21, 2018; DOI: 10.1158/2326-6066.CIR-18-0056

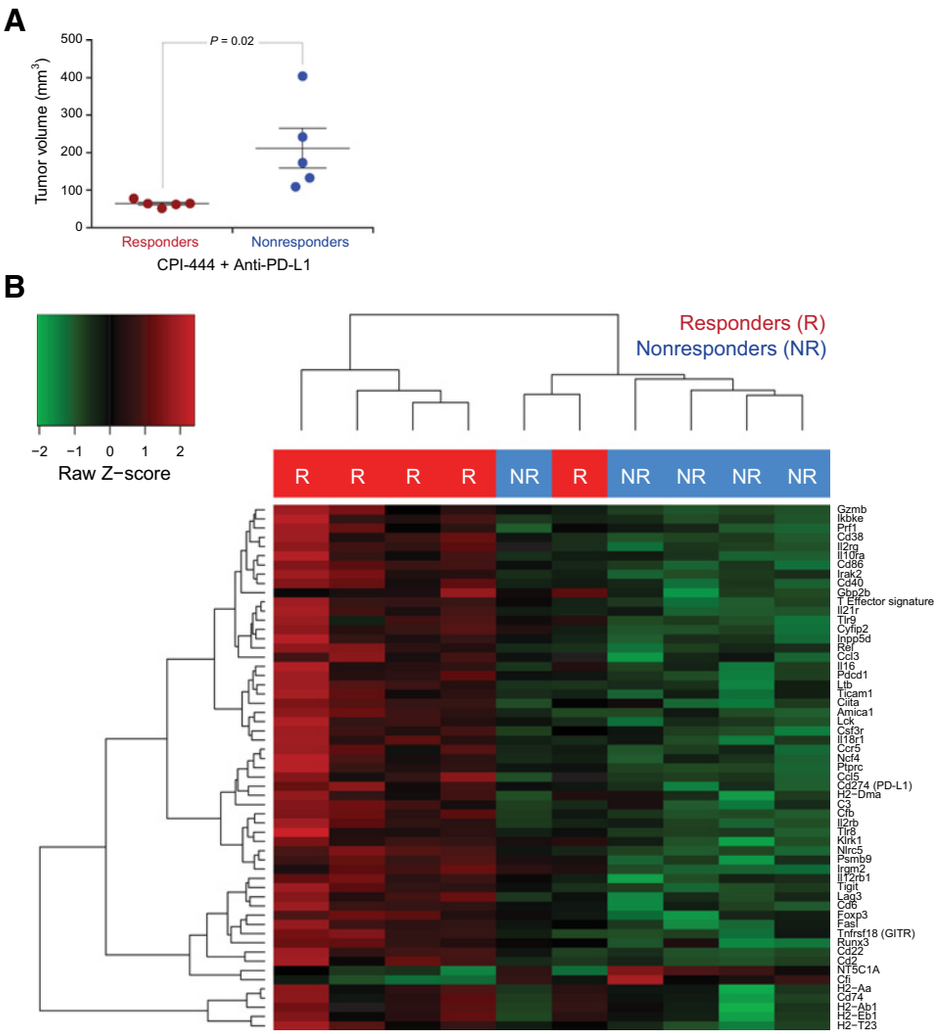

Figure 7.
Gene expression changes associated with response to combination CPI-444 and anti–PD-L1 treatment in MC38 tumors. **A,** Tumor volumes of responding ($n = 5$) and nonresponding ($n = 5$) MC38 tumors on day 17 post engraftment. Significance was calculated using unpaired Student *t* tests. **B,** RNA from responding (R) and nonresponding (NR) tumors treated with combination CPI-444 (100 mg/kg) and anti–PD-L1 (200 μg) was assayed using the NanoString PanCancer Immune Panel. All genes with raw *P* value less than 0.01 are shown. Positive fold-change values represent genes with higher expression in responding samples.

growth, and enabled antitumor immune memory. CPI-444 efficacy alone and in combination with anti–PD-L1 was associated with T-cell infiltration and an induction of a Th1 gene expression signature. CD73 expression was also increased in treated animals, revealing a potential resistance mechanism to CPI-444 and anti–PD-L1 treatment. These preclinical findings have been observed in patients treated with CPI-444 alone and in combination with anti–PD-L1 (atezolizumab), including patients who previously failed anti–PD-L1 therapy (44, 45). Expression of the adenosine pathway, including A2AR, CD73, and CD39, was shown to be significantly increased in patients who failed to respond to prior anti–PD-L1 blockade, supporting the hypothesis that adenosine signaling is a potential resistance mechanism to anti–PD-L1 treatment (45). Increases in T-cell infiltration were observed across multiple $CD73^+$ tumors treated with CPI-444, as well as a significant induction of immune checkpoints associated with IFNγ signaling (CXCL9 and CXCL10), effector function (GZMA and GZMB), and immune regulation (IDO1 and LAG3; ref. 45). Evidence of immune activation has also been observed in the periphery (44). CPI-444 treatment can induce substantial changes in the TCR repertoire in treated patients, including the generation of multiple novel, potentially tumor neoantigen-specific TCR clones (46). Our data clearly demonstrate immune modulation and antitumor responses in mice and human patients with cancer receiving an A2AR antagonist.

These results add to a well-established precedent for pharmacologic blockade of A2AR in oncology, either as single agent or combined with other checkpoint inhibitors (13, 26–32). We typically started dosing CPI-444 at the same time as anti–PD-L1 or anti–CTLA-4 treatment. Experiments exploring the sequence and timing of treatment are ongoing. In the preclinical studies reported here, CPI-444 potentiated antitumor responses in mice that otherwise failed to completely respond to anti–PD-L1 treatment. The mechanisms by which A2AR blockade overcomes anti–PD-L1 resistance are under investigation, but these results suggest that blockade of adenosine signaling may also enable antitumor responses in patients that previously failed anti–PD-L1 immunotherapy. Prior observations that anti–PD-1 treatment increased A2AR and CD73 expression suggest that CPI-444 may neutralize adenosine signaling that would otherwise actively limit immune responses following

anti–PD-L1 treatment (28, 29). This idea is consistent with reports from Beavis and colleagues demonstrating increased IFNγ production upon dual blockade of A2AR and PD-1 (29). Notably, others have shown that inhibiting A2AR signaling does not increase PD-1 or PD-L1 expression and may even decrease PD-1 on TILs (29, 40). Blockade of A2AR with CPI-444 also enabled us to decrease the effective dose of anti–PD-1 and anti–CTLA-4, while preserving efficacy in the CT26 mouse tumor model. These findings may be particularly applicable in mitigating the increase in treatment-related adverse events (grade 3 or 4) observed in patients with melanoma treated with nivolumab plus ipilimumab (55% compared with 16.3% of nivolumab or 27.3% of ipilimumab; ref. 41).

Expression of CD73 in the TME appears to influence the therapeutic activity of A2AR antagonists in preclinical models (10, 26, 29). In our studies, we observed that blockade of A2AR with CPI-444 may induce a compensatory increase in CD73 expression within the TME, presumably as a mechanism to increase adenosine and reassert immune suppression. These results are similar to those reported by Young and colleagues and suggest that dual targeting of A2AR and CD73 may further enhance antitumor responses (47). Such an approach has already been shown to be beneficial in limiting tumor growth and metastasis in mouse models (47). We also observed that anti–PD-L1 treatment induced CD73 expression as a potential adaptive resistance mechanism. Similar observations of increased CD73 expression have been observed in multiple patients' tumors following anti–PD-1 treatment in clinical trials (45, 48). It is possible that adenosine in some tumors can be elevated to the point that substantial signaling through the low-affinity A2B receptor becomes engaged (21). In this scenario, simultaneous blockade of A2AR and A2BR may be required to fully restore antitumor immunity, as A2BR signaling has been shown to limit myeloid cell immune responses. However, the relatively low concentrations of adenosine in the tumor models studied here indicated that signaling through the A2BR is not significant, and blockade of this receptor is unlikely to further enhance tumor immunity. The influence of A2AR, A2BR, and CD73 expression on CPI-444 treatment efficacy is currently being evaluated in patient matched pre- and posttreatment tumor biopsies and PBMC specimens collected in our clinical study.

Here, we reported that free extracellular adenosine concentrations were approximately 100–150 nmol/L in subcutaneously engrafted MC38 and CT26 tumors. This result is similar to the values reported by Blay and colleagues but are lower than estimates of 10–100 μmol/L proposed by others (14). The microdialysis method utilized in this study enabled an accurate, *in situ*, continuous measurement of extracellular adenosine in the TME. This method avoided the use of exogenous adenosine catabolism inhibitors that block adenosine degradation and transport (plasma $t_{1/2} \leq 10$ seconds) resulting in artificially elevated measurements by allowing adenosine to accumulate in the sample (49). This method does not rely on mechanical or enzymatic tissue disruption that results in potential overestimation of extracellular adenosine by including the adenosine generated upon release of intracellular adenine nucleotide stores into the extracellular milieu. Future studies will focus on evaluating adenosine in additional tumor models, including orthotopically engrafted tumors and genetically engineered tumor models that may more closely resemble the natural evolution of a suppressive microenvironment. We propose the well precedented *in vivo* microdialysis methodology be adopted by all investigators developing adenosine pathway modulators or in studies with potential therapeutic partners that may perturb adenosine in the TME (50).

In total, this work showed that CPI-444 is a potent and selective A2AR antagonist that enabled antitumor immunity in preclinical tumor models. On the basis of these results and others, we are conducting a phase I/Ib clinical trial (NCT02655822) to examine safety, tolerability, biomarkers, and efficacy of CPI-444 as a single agent and in combination with the anti–PD-L1 antibody, atezolizumab, in patients with non–small cell lung, melanoma, renal, triple-negative breast, and other (bladder, prostate, head and neck, colorectal) advanced tumors.

Disclosure of Potential Conflicts of Interest

S.B. Willingham is a senior scientist and has ownership interest in Corvus Pharmaceuticals. A. Hotson has ownership interest in Corvus Pharmaceuticals. C.M. Hill is an associate director and has ownership interest in Corvus Pharmaceuticals. E.C. Piccione is a senior scientist II at Corvus Pharmaceuticals. R.A. Miller is CEO, reports receiving a commercial research funding from, and has ownership interest in Corvus Pharmaceuticals. No potential conflicts of interest were disclosed by the other authors.

Authors' Contributions

Conception and design: S.B. Willingham, P.Y. Ho, C.M. Hill, I. McCaffery, R.A. Miller

Development of methodology: S.B. Willingham, P.Y. Ho, E.C. Piccione, L. Liu, I. McCaffery, R.A. Miller

Acquisition of data (provided animals, acquired and managed patients, provided facilities, etc.): P.Y. Ho, A. Hotson, E.C. Piccione, J. Hsieh, L. Liu, I. McCaffery, R.A. Miller

Analysis and interpretation of data (e.g., statistical analysis, biostatistics, computational analysis): S.B. Willingham, P.Y. Ho, A. Hotson, C.M. Hill, E.C. Piccione, I. McCaffery, R.A. Miller

Writing, review, and/or revision of the manuscript: S.B. Willingham, P.Y. Ho, A. Hotson, C.M. Hill, E.C. Piccione, J. Hsieh, L. Liu, J.J. Buggy, I. McCaffery, R.A. Miller

Administrative, technical, or material support (i.e., reporting or organizing data, constructing databases): P.Y. Ho, J. Hsieh, R.A. Miller

Study supervision: S.B. Willingham, C.M. Hill, L. Liu, J.J. Buggy, I. McCaffery, R.A. Miller

Other (investigated, evaluated, and interpreted the PK/PD relationship): L. Liu

Acknowledgments

We thank Leiv Lea, Brandon Dezewiecki, Victoria Dominguez, Ting Wang, Katherine Woodward, and Ran Xiao for administrative support. We thank Felicia Flicker and Jingrong Xu for support with formulations and preparation of reagents. We thank Carmen Choy, James Janc, Ben Jones, Long Kwei, Ginna Laport, Zhihong Li, Brian Munneke, Patrick Ng, and Erik Verner for scientific advice, technical support, and thoughtful discussion. We thank J. Ireland for bioinformatics support, and Florentino San Pablo and Timothy Velilla for assistance with animal experiments and animal care. We also thank Drs. Jonathan Powell and Robert Leone at Johns Hopkins Sidney Kimmel Cancer Center for thoughtful discussions.

The costs of publication of this article were defrayed in part by the payment of page charges. This article must therefore be hereby marked *advertisement* in accordance with 18 U.S.C. Section 1734 solely to indicate this fact.

Received February 5, 2018; revised June 12, 2018; accepted August 17, 2018; published first August 21, 2018.

Published OnlineFirst August 21, 2018; DOI: 10.1158/2326-6066.CIR-18-0056

References

1. Smyth MJ, Ngiow SF, Ribas A, Teng MW. Combination cancer immunotherapies tailored to the tumour microenvironment. Nat Rev Clin Oncol 2016;13:143–58.
2. Ohta A, Sitkovsky M. Role of G-protein-coupled adenosine receptors in downregulation of inflammation and protection from tissue damage. Nature 2001;414:916–20.
3. Hasko G, Linden J, Cronstein B, Pacher P. Adenosine receptors: therapeutic aspects for inflammatory and immune diseases. Nat Rev Drug Discov 2008;7:759–70.
4. Leone RD, Lo YC, Powell JD. A2aR antagonists: Next generation checkpoint blockade for cancer immunotherapy. Comput Struct Biotechnol J 2015;13:265–72.
5. Young A, Mittal D, Stagg J, Smyth MJ. Targeting cancer-derived adenosine: new therapeutic approaches. Cancer Discov 2014;4:879–88.
6. Allard D, Turcotte M, Stagg J. Targeting A2 adenosine receptors in cancer. Immunol Cell Biol 2017;95:333–9.
7. Antonioli L, Blandizzi C, Pacher P, Haskó G. Immunity, inflammation and cancer: a leading role for adenosine. Nat Rev Cancer 2013;13:842–57.
8. Junger WG. Immune cell regulation by autocrine purinergic signalling. Nat Rev Immunol 2011;11:201–12.
9. Beavis PA, Henderson MA, Giuffrida L, Mills JK, Sek K, Cross RS, et al. Targeting the adenosine 2A receptor enhances chimeric antigen receptor T cell efficacy. J Clin Invest 2017;127:929–41.
10. Loi S, Pommey S, Haibe-Kains B, Beavis PA, Darcy PK, Smyth MJ, et al. CD73 promotes anthracycline resistance and poor prognosis in triple negative breast cancer. Proc Natl Acad Sci USA 2013;110:11091–6.
11. Hatfield SM, Kjaergaard J, Lukashev D, Schreiber TH, Belikoff B, Abbott R, et al. Immunological mechanisms of the antitumor effects of supplemental oxygenation. Sci Transl Med 2015;7:277ra30.
12. Synnestvedt K, Furuta GT, Comerford KM, Louis N, Karhausen J, Eltzschig HK, et al. Ecto-5′-nucleotidase (CD73) regulation by hypoxia-inducible factor-1 mediates permeability changes in intestinal epithelia. J Clin Invest 2002;110:993–1002.
13. Ohta A, Gorelik E, Prasad SJ, Ronchese F, Lukashev D, Wong MK, et al. A2A adenosine receptor protects tumors from antitumor T cells. Proc Natl Acad Sci USA 2006;103:13132–7.
14. Blay J, White TD, Hoskin DW. The extracellular fluid of solid carcinomas contains immunosuppressive concentrations of adenosine. Cancer Res 1997;57:2602–5.
15. Tak E, Jung DH, Kim SH, Park GC, Jun DY, Lee J, et al. Protective role of hypoxia-inducible factor-1alpha-dependent CD39 and CD73 in fulminant acute liver failure. Toxicol Appl Pharmacol 2017;314:72–81.
16. Sitkovsky MV. T regulatory cells: hypoxia-adenosinergic suppression and re-direction of the immune response. Trends Immunol 2009;30:102–8.
17. Mandapathil M, Hilldorfer B, Szczepanski MJ, Czystowska M, Szajnik M, Ren J, et al. Generation and accumulation of immunosuppressive adenosine by human CD4+CD25highFOXP3+ regulatory T cells. J Biol Chem 2010;285:7176–86.
18. Maj T, Wang W, Crespo J, Zhang H, Wang W, Wei S, et al. Oxidative stress controls regulatory T cell apoptosis and suppressor activity and PD-L1-blockade resistance in tumor. Nat Immunol 2017;18:1332–41.
19. Dong RP, Kameoka J, Hegen M, Tanaka T, Xu Y, Schlossman SF, et al. Characterization of adenosine deaminase binding to human CD26 on T cells and its biologic role in immune response. J Immunol 1996;156:1349–55.
20. Antonioli L, Fornai M, Colucci R, Ghisu N, Tuccori M, Del Tacca M, et al. Regulation of enteric functions by adenosine: pathophysiological and pharmacological implications. Pharmacol Ther 2008;120:233–53.
21. de Lera Ruiz M, Lim YH, Zheng J. Adenosine A2A receptor as a drug discovery target. J Med Chem 2014;57:3623–50.
22. Clayton A, Al-Taei S, Webber J, Mason MD, Tabi Z. Cancer exosomes express CD39 and CD73, which suppress T cells through adenosine production. J Immunol 2011;187:676–83.
23. Hasko G, Pacher P. Regulation of macrophage function by adenosine. Arterioscler Thromb Vasc Biol 2012;32:865–9.
24. Novitskiy SV, Ryzhov S, Zaynagetdinov R, Goldstein AE, Huang Y, Tikhomirov OY, et al. Adenosine receptors in regulation of dendritic cell differentiation and function. Blood 2008;112:1822–31.
25. Csoka B, Himer L, Selmeczy Z, Vizi ES, Pacher P, Ledent C, et al. Adenosine A2A receptor activation inhibits T helper 1 and T helper 2 cell development and effector function. FASEB J 2008;22:3491–9.
26. Mittal D, Young A, Stannard K, Yong M, Teng MW, Allard B, et al. Antimetastatic effects of blocking PD-1 and the adenosine A2A receptor. Cancer Res 2014;74:3652–8.
27. Iannone R, Miele L, Maiolino P, Pinto A, Morello S. Adenosine limits the therapeutic effectiveness of anti-CTLA4 mAb in a mouse melanoma model. Am J Cancer Res 2014;4:172–81.
28. Allard B, Pommey S, Smyth MJ, Stagg J. Targeting CD73 enhances the antitumor activity of anti-PD-1 and anti-CTLA-4 mAbs. Clin Cancer Res 2013;19:5626–35.
29. Beavis PA, Milenkovski N, Henderson MA, John LB, Allard B, Loi S, et al. Adenosine receptor 2A blockade increases the efficacy of anti-PD-1 through enhanced antitumor T-cell responses. Cancer Immunol Res 2015;3:506–17.
30. Waickman AT, Alme A, Senaldi L, Zarek PE, Horton M, Powell JD. Enhancement of tumor immunotherapy by deletion of the A2A adenosine receptor. Cancer Immunol Immunother 2012;61:917–26.
31. Beavis PA, Divisekera U, Paget C, Chow MT, John LB, Devaud C, et al. Blockade of A2A receptors potently suppresses the metastasis of CD73+ tumors. Proc Natl Acad Sci U S A 2013;110:14711–6.
32. Beavis PA, Milenkovski N, Stagg J, Smyth MJ, Darcy PK. A2A blockade enhances anti-metastatic immune responses. Oncoimmunology 2013;2:e26705.
33. Sitkovsky MV, Hatfield S, Abbott R, Belikoff B, Lukashev D, Ohta A. Hostile, hypoxia-A2-adenosinergic tumor biology as the next barrier to overcome for tumor immunologists. Cancer Immunol Res 2014;2:598–605.
34. Lutty GA, Mathews MK, Merges C, McLeod DS. Adenosine stimulates canine retinal microvascular endothelial cell migration and tube formation. Curr Eye Res 1998;17:594–607.
35. Montesinos MC, Desai A, Chen JF, Yee H, Schwarzschild MA, Fink JS, et al. Adenosine promotes wound healing and mediates angiogenesis in response to tissue injury via occupancy of A(2A) receptors. Am J Pathol 2002;160:2009–18.
36. Ohta A, Ohta A, Madasu M, Kini R, Subramanian M, Goel N, et al. A2A adenosine receptor may allow expansion of T cells lacking effector functions in extracellular adenosine-rich microenvironments. J Immunol 2009;183:5487–93.
37. Yang A, Mucsi AD, Desrosiers MD, Chen JF, Schnermann JB, Blackburn MR, et al. Adenosine mediated desensitization of cAMP signaling enhances T-cell responses. Eur J Immunol 2010;40:449–59.
38. Koshiba M, Rosin DL, Hayashi N, Linden J, Sitkovsky MV. Patterns of A2A extracellular adenosine receptor expression in different functional subsets of human peripheral T cells. Flow cytometry studies with anti-A2A receptor monoclonal antibodies. Mol Pharmacol 1999;55:614–24.
39. Bshesh K, Zhao B, Spight D, Biaggioni I, Feokistov I, Denenberg A, et al. The A2A receptor mediates an endogenous regulatory pathway of cytokine expression in THP-1 cells. J Leukoc Biol 2002;72:1027–36.
40. Cekic C, Linden J. Adenosine A2A receptors intrinsically regulate CD8+ T cells in the tumor microenvironment. Cancer Res 2014;74:7239–49.
41. Larkin J, Chiarion-Sileni V, Gonzalez R, Grob JJ, Cowey CL, Lao CD, et al. Combined nivolumab and ipilimumab or monotherapy in untreated melanoma. N Engl J Med 2015;373:23–34.
42. Postow MA, Chesney J, Pavlick AC, Robert C, Grossmann K, McDermott D, et al. Nivolumab and ipilimumab versus ipilimumab in untreated melanoma. N Engl J Med 2015;372:2006–17.
43. Zarek PE, Huang CT, Lutz ER, Kowalski J, Horton MR, Linden J, et al. A2A receptor signaling promotes peripheral tolerance by inducing T-cell anergy and the generation of adaptive regulatory T cells. Blood 2008;111:251–9.
44. Fong L, Forde PM, Powderly JD, Goldman JW, Nemunaitis JJ, Luke JJ. Safety and clinical activity of adenosine A2a receptor (A2aR) antagonist, CPI-444, in anti-PD1/PDL1 treatment-refractory renal cell (RCC) and non-small cell lung cancer (NSCLC) patients. J Clin Oncol 35:15s, 2017 (suppl; abstr 3004).
45. Hotson A, et al. Clinical Activity of Adenosine 2A Receptor (A2AR) Inhibitor CPI-444 is Associated with Tumor Expression of Adenosine Pathway Genes and Tumor Immune Modulation. in Society for Immunotherapy of Cancer Annual Meeting. 2017. National Harbon, Maryland, USA. http:/ www.sitcancer.org/2017/abstracts/info

Published OnlineFirst August 21, 2018; DOI: 10.1158/2326-6066.CIR-18-0056

46. Willingham S, et al. Abstract 5593: Inhibition of A2AR induces anti-tumor immunity alone and in combination with anti-PD-L1 in preclinical and clinical studies. Cancer Res 2017;77(13 Supplement):5593.
47. Young A, Ngiow SF, Barkauskas DS, Sult E, Hay C, Blake SJ, et al. Co-inhibition of CD73 and A2AR adenosine signaling improves anti-tumor immune responses. Cancer Cell 2016;30:391–403.
48. Reinhardt J, Landsberg J, Schmid-Burgk JL, Ramis BB, Bald T, Glodde N, et al. MAPK signaling and inflammation link melanoma phenotype switching to induction of CD73 during immunotherapy. Cancer Res 2017;77:4697–709.
49. Moser GH, Schrader J, Deussen A. Turnover of adenosine in plasma of human and dog blood. Am J Physiol 1989;256(4 Pt 1):C799–806.
50. Ramakers BP, Pickkers P, Deussen A, Rongen GA, van den Broek P, van der Hoeven JG, et al. Measurement of the endogenous adenosine concentration in humans in vivo: methodological considerations. Curr Drug Metab 2008;9:679–85.

Published OnlineFirst August 21, 2018; DOI: 10.1158/2326-6066.CIR-18-0056

Cancer Immunology Research

A2AR Antagonism with CPI-444 Induces Antitumor Responses and Augments Efficacy to Anti –PD-(L)1 and Anti–CTLA-4 in Preclinical Models

Stephen B. Willingham, Po Y. Ho, Andrew Hotson, et al.

Cancer Immunol Res 2018;6:1136-1149. Published OnlineFirst August 21, 2018.